






Unexpected Mechanism of Biodegradation and Defluorination of 2,2-Difluoro-1,3-Benzodioxole by *Pseudomonas putida* F1

 Madison D. Bygd,^a  Kelly G. Aukema,^{b,c} Jack E. Richman,^{b,c}  Lawrence P. Wackett^{b,c}

^aMicrobial Engineering, University of Minnesota, St. Paul, Minnesota, USA

^bBiochemistry, Molecular Biology and Biophysics, University of Minnesota, St. Paul, Minnesota, USA

^cBioTechnology Institute, University of Minnesota, St. Paul, Minnesota, USA

ABSTRACT Perfluorinated carbon atoms in a diether linkage are common in commercial anesthetics, drugs, fungicides, and insecticides. An important chemical group comprising perfluorodiethers is the 2,2-fluoro-1,3-benzodioxole (DFBD) moiety. The fluorine atoms stabilize the molecule by mitigating against metabolism by humans and microbes, as used in drugs and pesticides, respectively. *Pseudomonas putida* F1 catalyzed defluorination of DFBD at an initial rate of 2,100 nmol/h per mg cellular protein. This is orders of magnitude higher than previously reported microbial defluorination rates with multiply fluorinated carbon atoms. Defluorination rates declined after several hours, and the medium darkened. Significant defluorination activity was observed with cells grown on toluene but not L-arginine. Defluorination required only toluene dioxygenase. *Pseudomonas* and recombinant *Escherichia coli* cells expressing toluene dioxygenase oxidized DFBD to DFBD-4,5-dihydrodiol. The dihydrodiol could be oxidized to 4,5-dihydroxy-DFBD via the dihydrodiol dehydrogenase from *P. putida* F1. The dihydrodiol dehydrated with acid to yield a mixture of 4-hydroxy-DFBD and 5-hydroxy-DFBD. All those metabolites retained the difluoromethylene group; no fluoride or dark color was observed. The major route of DFBD-4,5-dihydrodiol decomposition produced fluoride and 1,2,3-trihydroxybenzene, or pyrogallol, and that was shown to be the source of the dark colors in the medium. A mechanism for DFBD-4,5-dihydrodiol transformation to two fluoride ions and pyrogallol is proposed. The *Pseudomonas* genome database and other databases revealed hundreds of bacteria with enzymes sharing high amino acid sequence identity to toluene dioxygenase from *P. putida* F1, suggesting the mechanism revealed here may apply to the defluorination of DFBD-containing compounds in the environment.

IMPORTANCE There are more than 9,000 polyfluorinated compounds developed for commercial use, some negatively impacting human health, and they are generally considered to be resistant to biodegradation. Only a limited number of studies have identified microbes with enzymes sufficiently reactive to defluorinate difluoromethylene carbon groups. The present study examined one important group of commercial fluorinated chemicals and showed its rapid defluorination by a bacterium and its key enzyme, a Rieske dioxygenase. Rieske dioxygenases are common in environmental bacteria, and those closely resembling toluene dioxygenase from *Pseudomonas putida* F1 are candidates for biodegradative defluorination of the common 2,2-fluoro-1,3-benzodioxole (DFBD) moiety.

KEYWORDS organofluorine, PFAS, defluorination, *Pseudomonas putida* F1, bacteria, dioxygenase, rapid rate, pyrogallol, fluoride, pesticides, oxygenase

Fluorinated organic compounds are considered to be one of the major foci of biodegradation currently because of their prevalence, emerging concerns about health effects, and their prolonged lifetime in the environment (1). Naturally occurring

Citation Bygd MD, Aukema KG, Richman JE, Wackett LP. 2021. Unexpected mechanism of biodegradation and defluorination of 2,2-difluoro-1,3-benzodioxole by *Pseudomonas putida* F1. mBio 12:e03001-21. <https://doi.org/10.1128/mBio.03001-21>.

Editor Caroline S. Harwood, University of Washington

Copyright © 2021 Bygd et al. This is an open-access article distributed under the terms of the [Creative Commons Attribution 4.0 International license](https://creativecommons.org/licenses/by/4.0/).

Address correspondence to Lawrence P. Wackett, wacke003@umn.edu.

This article is a direct contribution from Lawrence P. Wackett, a Fellow of the American Academy of Microbiology, who arranged for and secured reviews by William Mohn, University of British Columbia, and Victor de Lorenzo, Centro Nacional de Biotecnología.

Received 11 October 2021

Accepted 12 October 2021

Published 16 November 2021

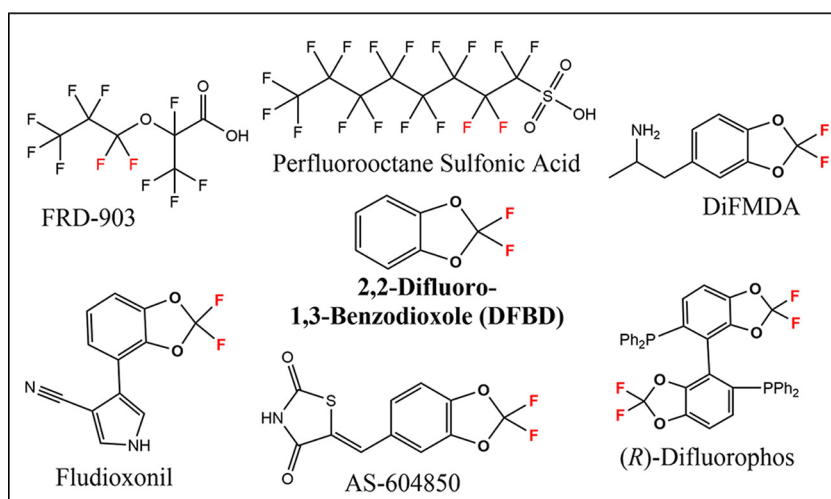


FIG 1 Examples of commercially relevant polyfluorinated compounds. The center compound in bold is 2,2-difluoro-1,3-benzodioxole (DFBD). Compounds containing the DFBD moiety shown are the experimental drug DiFMDA (difluoromethylenedioxyamphetamine), the fungicide fludioxonil, the anticancer agent AS-604850, and the reagent for enantioselective synthesis (*R*)-difluorophos.

compounds with carbon-fluorine bonds are relatively rare, and most contain a single fluorine substituent (2–4). Synthetic, commercially important fluorinated compounds typically contain multiple fluorine atoms, and that makes them less reactive to defluorination, both chemically and biologically (5, 6). In light of that, there have been a limited number of studies demonstrating biodegradation of multiply fluorinated compounds. Recently, perfluorinated compounds have been shown to be biodegradable (7, 8) but the genes and enzymes involved in their defluorination are not yet known.

Difluorinated ethers are common in industrial chemicals, particularly in pharmaceutical and pesticidal compounds. They are of particular interest currently with the introduction of 2,3,3,3-tetrafluoro-2-(heptafluoropropoxy)propanoic acid, commonly known as FRD-903, as a substitute for other perfluorinated alkyl substances (PFAS) such as perfluorooctane sulfonic acid (Fig. 1). A common and emerging class of difluoro ether compounds contains the 2,2-difluoro-1,3-benzodioxole (DFBD) group (9, 10). Commercial DFBD-containing compounds include the fungicide fludioxonil, the anticancer therapeutic AS-604850, the synthetic reagent (*R*)-difluorophos, and the experimental drug difluoromethylenedioxyamphetamine (DiFMDA) (Fig. 1). Many other DFBD-based difluoroethers are in commercial use currently (11). The difluoromethylene group is designed into ring structures because it prolongs the lifetime of the compounds in both the human body and the environment. DFBD-containing pesticides are considered to be moderately recalcitrant, with several studies using enrichments from soil and water showing their disappearance in days to weeks (12, 13). However, those studies did not identify the genes or enzymes responsible for the metabolism.

The defluorination of difluoromethylene carbons in ether linkages is not well studied, and DFBD provides an excellent model for developing understanding. It remains to be established if the fluorines would be displaceable via hydrolytic, reductive, or other mechanisms. The difluorinated carbon atom in DFBD is also bonded to two oxygen atoms. As such, it is completely oxidized and unlikely to undergo oxidative defluorination directly. Defluorination by oxidizing enzymes such as oxygenases is known (14, 15), typically with a carbon atom bonded to a single fluorine atom, unlike in DFBD (16–19). Perfluoroethylene is biodegraded to defluorinated products by soluble methane monooxygenase from *Methylosinus trichosporium* Ob3B (20). Recently, an elimination mechanism has been proposed to initiate the biodegradation of 3,3,3-trifluoropropionic acid (21), but this mechanism would not apply to the DFBD difluoro-diether group.

For more insights into DFBD defluorination, we chose to examine model *Pseudomonas* strains for which genomes are available and enzymes have been purified and characterized. The first defluorinating enzyme studied, fluoroacetate defluorinase, was purified and characterized from a *Pseudomonas* strain (22). In one recent study, fluoroacetate was shown to undergo defluorination by multiple bacterial strains, but difluoro- and trifluoroacetates were uniformly recalcitrant (23). However, *Pseudomonas* strains are known to contain organochlorine dehalogenases that react with dichloro- and trichloro- substrates (24, 25). Moreover, *Pseudomonas* genomes are known to encode >25% proteins of unknown function, suggesting novel defluorinating activities may yet be discovered (26, 27). After initially screening several *Pseudomonas* strains against a small library of fluorinated compounds, we observed significant levels of fluoride anion in the medium with strain *Pseudomonas putida* F1 and DFBD. This model strain has had its genome sequenced and multiple enzymes characterized in detail (28, 29). The most well-studied enzymes are involved in the metabolism of aromatic hydrocarbons (30), and DFBD contains an aromatic ring. Moreover, the DFBD moiety is known to be quite stable, underlying its incorporation into numerous commercial products (Fig. 1).

The present study focused on DFBD transformation by *P. putida* F1 and the mechanism by which free fluoride was released into the medium. Using the combined tools of nuclear magnetic resonance (NMR) spectroscopy, gas chromatography (GC), and mass spectrometry (MS), we propose here a novel mechanism underlying fluoride displacement from the DFBD group. It was demonstrated that the only enzyme required for defluorination of DFBD is toluene dioxygenase, and the mechanism elucidated here has, to our knowledge, never been shown previously. Moreover, many environmental bacteria express toluene dioxygenase homologs, suggesting that the mechanism revealed here may be operative with DFBD compounds found in soil and water.

RESULTS AND DISCUSSION

Metabolic studies with wild-type *Pseudomonas putida* F1. Wild-type cells of *P. putida* F1 were grown to mid-exponential phase on toluene vapors to induce toluene dioxygenase and related enzymes. The toluene vapor was removed and replaced with 2,2-difluoro-1,3-benzodioxole (DFBD) vapor, and free fluoride ion was detected immediately. Over time, color change of the medium was also observed (see Fig. S1 in the supplemental material). The release of free fluoride ion was measured using a fluoride electrode, which showed a rapid accumulation of fluoride in the first 4 h (Fig. 2A). After this, fluoride in the medium plateaued at ~1 mM, which was followed by a darkening of the medium (Fig. 2B). Cells grown on L-arginine as a carbon source that were not induced with toluene produced minimal levels of fluoride (0.1 mM over 24 h). Additionally, DFBD was stable in medium in the absence of cells. No fluoride was released, and there was no darkening of medium. When sodium fluoride was added to medium, no color change was observed. In multiple experiments, color change was always linked to fluoride release but lagged behind temporally as shown in Fig. 2.

The initial rate of fluoride ion release was 2,100 nmol/h per mg of cell protein. By way of comparison, the rates of initial enzymatic attack on toluene by different *Pseudomonas* strains are reported to range from 720 to 10,800 nmol/h per mg protein (31). Defluorination of difluoromethylene carbon atoms by microorganisms has rarely been reported, and when it has, it is typically orders of magnitude slower and measured over weeks or months (7, 8). The rapid plateau reached after 4 h suggests that some factor becomes limiting. This argues against a hydrolytic defluorination since that would require only water that would not become limiting. The observations are more consistent with a redox reaction, since NADH or other sources of electrons could conceivably become depleted. The observation that growth on toluene is required suggests a role for one or more components of the toluene metabolic pathway.

Metabolic studies with mutant *P. putida* F39/D and *Escherichia coli* (pDTG601a) expressing toluene dioxygenase. The observations with wild-type *P. putida* F1 suggested that one or more components of the toluene degradation pathway were involved in DFBD defluorination and the darkening of the medium. Since the pathway is initiated

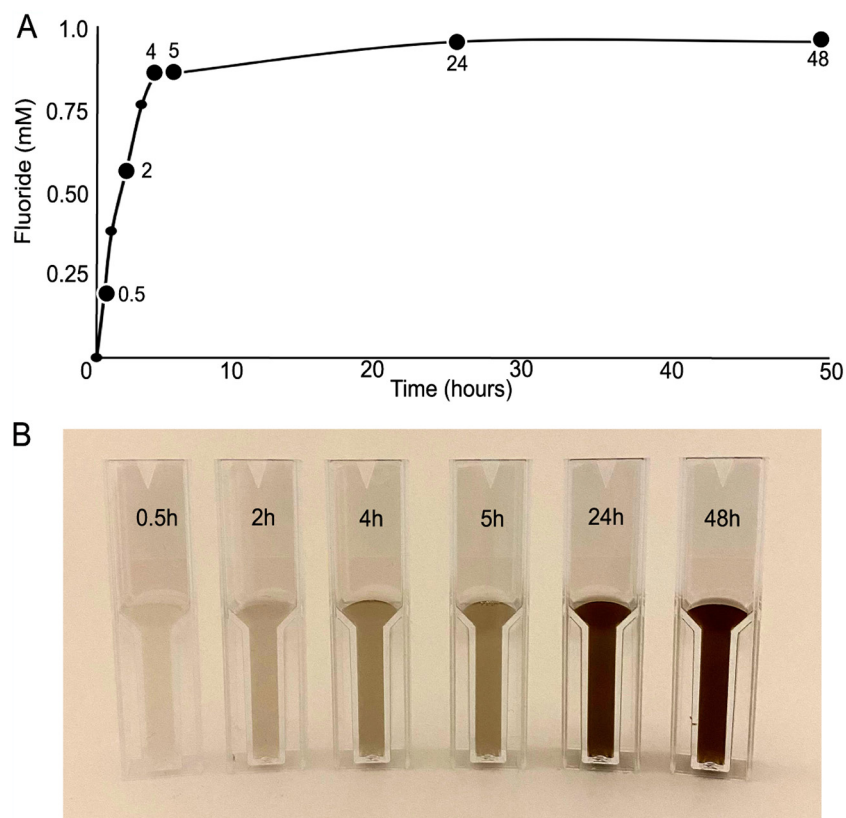


FIG 2 Fluoride release (A) and color change (B) in medium of a culture of *Pseudomonas putida* F1 incubated with DFBD with shaking over 48 h. *P. putida* F1 was grown with toluene as the carbon source, which induces the toluene catabolic pathway, and then the culture was switched to DFBD. For fluoride measurements, cells were removed, and the supernatant liquid was analyzed for fluoride, using an ion-specific electrode, as shown in panel A. Aliquots of the culture were taken at the times indicated and stored frozen, and then all were directly photographed, as shown in panel B.

by toluene dioxygenase (TDO), we first aimed to examine that enzyme's reaction with DFBD in isolation. Toluene dioxygenase consists of three components that are highly unstable and separate upon cell lysis and purification. They are a flavoprotein reductase (TodA), a ferredoxin (TodB), and the Rieske dioxygenase protein (TodC₁C₂) (32). So, an *in vivo* approach was pursued with *P. putida* F39/D, a derivative of *P. putida* F1 that lacks a functional second enzyme in the toluene catabolic pathway (33), and the recombinant strain *E. coli* (pDTG601a), which contains the *todC1C2BA* genes encoding the complete TDO system but no other enzymes of the toluene pathway (29). It is plausible that these two systems could give different results. For example, the TodE catechol oxygenase in *P. putida* F39/D could hypothetically catalyze ring cleavage leading to defluorination and *E. coli* DTG601a does not contain that enzyme.

P. putida F39/D was grown on L-arginine and induced with toluene vapor before incubation with DFBD. *E. coli* (pDTG601a) was induced with isopropyl- β -D-thiogalactopyranoside (IPTG) and subsequently incubated with DFBD. In both cases, the media were extracted with ethyl acetate, concentrated using a rotary evaporator, and analyzed by GC-MS and NMR as described in Materials and Methods. The GC-MS and ¹⁹F-NMR analyses were both consistent with the formation of a 4,5-dihydro-2,2-difluoro-1,3-benzodioxole-4,5-diol (4,5-DD-DFBD) (Fig. 3). Similar results were obtained with the *P. putida* F39/D and *E. coli* (pDTG601a) extracts. Because dihydrodiols are subject to decomposition in high temperatures of the GC inlet, extracted medium was derivatized prior to GC-MS analysis. Both the GC retention time and the mass spectrum of the prominent peak at 12.64 min are consistent with its identification as a derivatized dihydrodiol (Fig. 3A and B). Further structural information was gained from ¹⁹F-NMR that

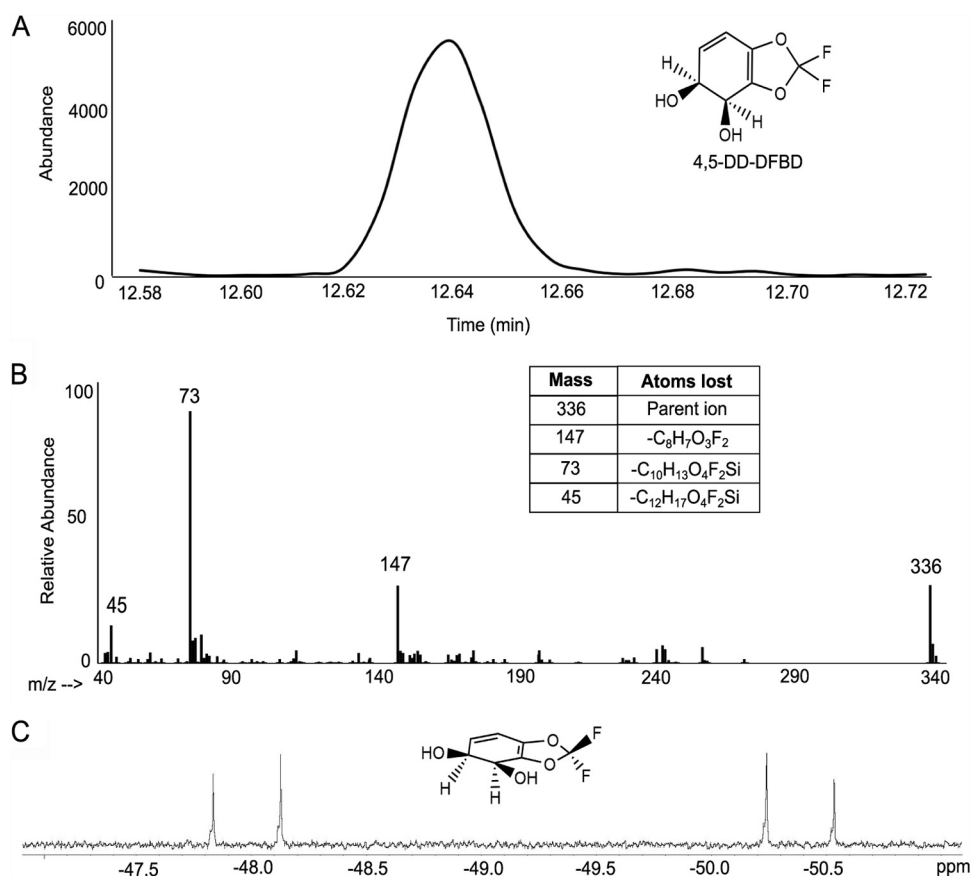


FIG 3 Toluene dioxygenase oxidation of DFBD to a *cis*-dihydrodiol. Analytical demonstration of 4,5-*cis*-dihydroxydihydro-2,2-difluoro-1,3-benzodioxole (4,5-DD-DFBD) by GC, MS, and NMR. The structure of the compound is shown in the upper right of panel A. The material analyzed by GC and MS was derivatized as detailed in Materials and Methods. While the data are consistent with a *cis*-dihydrodiol, the absolute stereochemistry has not been determined, and that shown is consistent with dihydrodiols produced by toluene dioxygenase. (A) Gas chromatogram of the extracted product derivatized with trimethylsilane. (B) Mass spectrum of the compound represented by the 12.64-min peak. The parent compound has an m/z of 336, and the $m/z = 337,338$ envelope is consistent with 1.1% natural abundance of ¹³C and a compound containing 13 carbon atoms. The disilyl fragment with an m/z of 147 is characteristic of compounds with two adjacent derivatized hydroxyl groups. (C) ¹⁹F-NMR spectrum at 400 MHz of 4,5-DD-DFBD. The two coupled doublets are consistent with two fluorines on differentiated faces, in this case arising from the *cis* configuration of the hydroxyl groups. The 3-dimensional depiction of 4,5-DD-DFBD illustrates the asymmetry imposed by the *cis*-dihydroxylation of DFBD.

showed that both fluorine atoms were retained in the product (Fig. 3C). The fluorine resonance splitting demonstrated that the plane of the benzene ring was asymmetric, consistent with a *cis*-dihydrodiol. The oxidation of bicyclic fused ring compounds, such as indan (34), by toluene dioxygenase has not been observed to produce bridgehead diols, and the enzyme consistently produces *cis*-dihydrodiols. Therefore, it was predicted that the *cis*-dihydrodiol being formed was most likely a 4,5-*cis*-dihydrodiol.

Dehydration of the *cis*-dihydrodiol-DFBD. It was decided that following the fate of 4,5-DD-DFBD would lead to insights into darkening of medium and the defluorination mechanism. Dihydrodiols are known to readily undergo dehydration to yield phenols. The dehydration reaction with substituted benzenes often produces a mixture of two phenols (33). The initial evidence that the DFBD dihydrodiol is unstable came from its low yield and subsequent NMR analysis, initially described in the previous section. When it was dried and taken up in CDCl₃, a solvent known to be slightly acidic, the ¹⁹F-NMR spectrum showed a collapse of the fluorine doublet into a single resonance, consistent with a rearomatization of the benzene ring that would occur with dehydration, producing a monohydroxylated aromatic ring (Fig. S6). With rearomatization, the environments of the two fluorine substituents become identical.

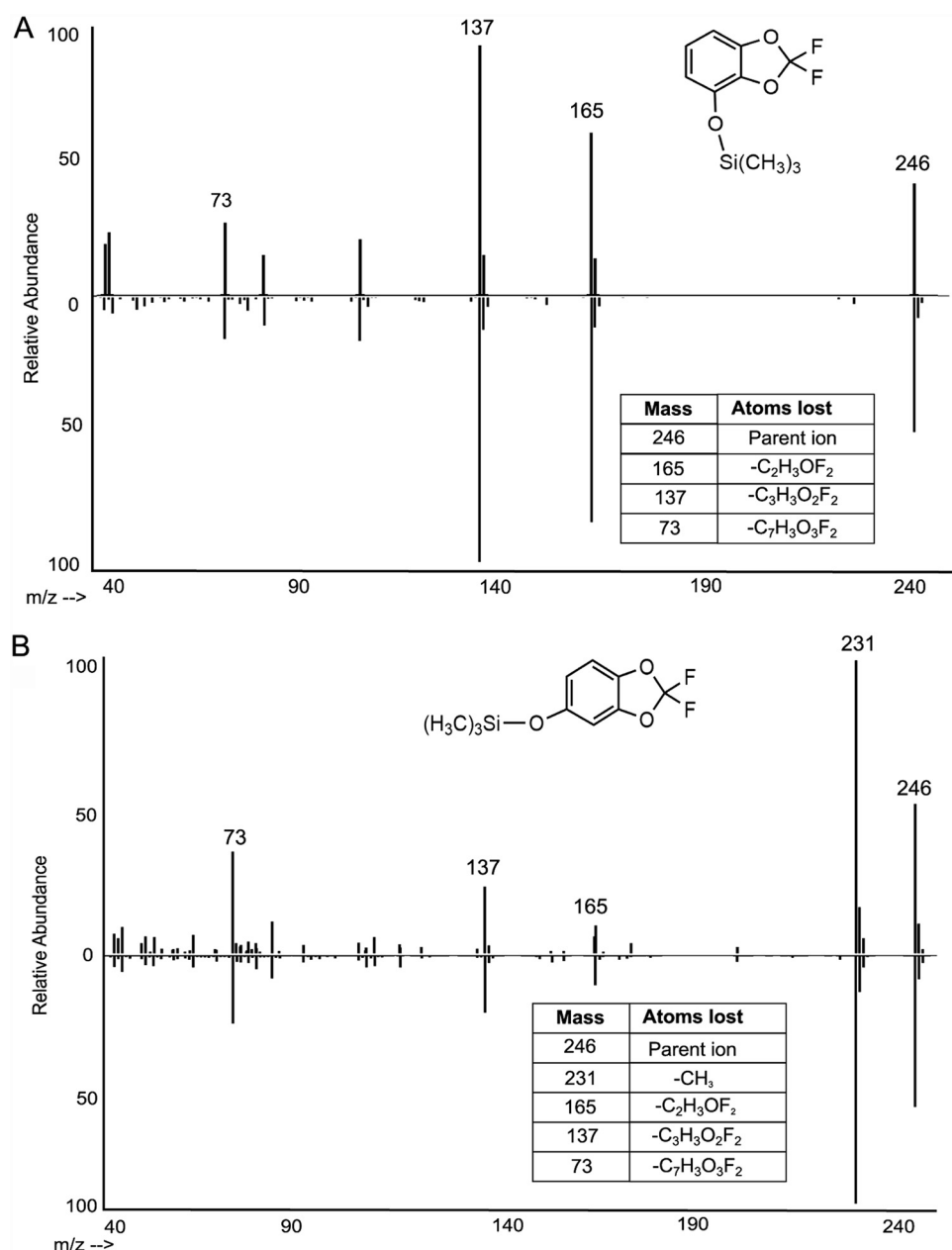


FIG 4 Comparison of dihydrodiol dehydration products from *E. coli* pDTG601a with synthetic standards following derivatization and mass spectrometry. (A) Mass spectra of trimethylsilane (TMS)-derivatized metabolite from cell cultures incubated with DFBD (top) and standard DFBD-4-ol (bottom). (B) Mass spectra of TMS-derivatized metabolite from cell cultures incubated with DFBD (top) and standard DFBD-5-ol (bottom).

From the NMR spectrum, it could not be discerned whether DFBD-4-ol, DFBD-5-ol, or both are formed.

Direct evidence was obtained that both DFBD-4-ol and DFBD-5-ol form in growth medium. This was determined by GC-MS, following derivatization to make both trimethylsilyl derivatives, and in comparison to authentic standards of each (Fig. 4). Together, they are not major products and account for <20% of total products. Moreover, addition of DFBD-4-ol and DFBD-5-ol to *P. putida* F1 growth medium did not lead to formation of fluoride; both compounds are stable in medium. In addition, no evidence for the metabolism of standard DFBD-4-ol and DFBD-5-ol by *P. putida* F39/D or *E. coli* (pDTG601a) in minimal salts basal (MSB) medium was observed. Based on these observations, additional metabolic studies were needed to uncover the mechanism of fluoride displacement.

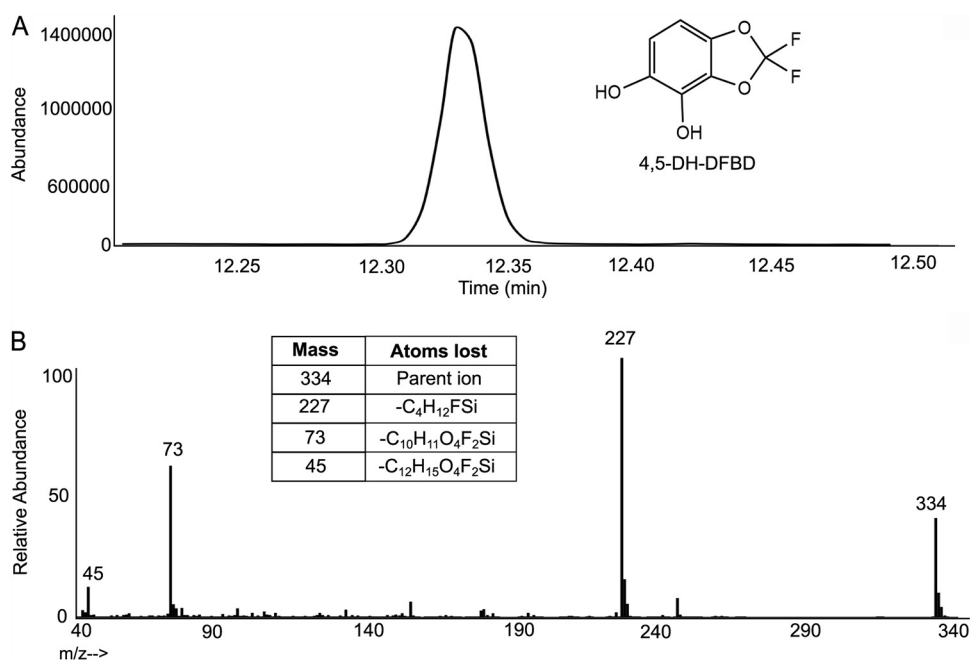


FIG 5 Extracted product derived from *E. coli* (pDTG602) expressing toluene dioxygenase and toluene dihydrodiol dehydrogenase. (A) Gas chromatogram of the compound identified as TMS-derivatized 4,5-dihydroxy-DFBD. (B) Mass spectrum of TMS-derivatized 4,5-dihydroxy-DFBD. The parent compound shows an m/z of 334.

***E. coli* (pDTG602) expressing toluene dioxygenase and diol dehydrogenase.** *P. putida* F1 is known to oxidize *cis*-dihydrodiols to catechols that can oxidize to form products that darken growth medium (29). In that context, we sought to accumulate the catechol from DFBD and determine if that could help explain medium darkening and fluoride release. The experiment used *E. coli* (pDTG602), which contains genes encoding toluene dioxygenase and dihydrodiol dehydrogenase and is known to accumulate catechols (29). This study produced a metabolite consistent with 4,5-dihydroxy-DFBD (4,5-DH-DFBD), as demonstrated by ¹H-NMR (Fig. S7), ¹⁹F-NMR (Fig. S8), and GC-MS after derivatization (Fig. 5). However, this intermediate also maintained the two fluorine substituents on the intact 1,3-dioxolane ring. This was confirmed via GC-MS (Fig. 5) and ¹⁹F-NMR (Fig. S8). Moreover, similar to the presence of DFBD-4-ol and DFBD-5-ol in *E. coli* (pDTG601a) cultures, 4,5-dihydroxy-DFBD was formed in only low yield. More importantly, we observed that medium from *E. coli* pDTG602 incubated with DFBD did darken but not as quickly or to the same extent with as with *P. putida* F39/D and *E. coli* (pDTG601a). This suggested that the DFBD-4,5-dihydrodiol is undergoing some other reaction to give a colored product(s) and fluoride.

Identification of pyrogallol, a defluorinated product that explained medium darkening. The volatility of DFBD prevented our determining the stoichiometry of DFBD oxidized to the amount of fluoride released. The initial rate of fluoride release (Fig. 2) was high, and the yields of DFBD-4-ol, DFBD-5-ol, and 4,5-DH-DFBD were low, suggesting that the DFBD-*cis*-4,5-dihydrodiol undergoes another reaction leading to defluorination. In this context, another organic product was sought in cultures of *E. coli* (pDTG601a) and *P. putida* F39/D. GC-MS revealed the transient formation of a nonfluorinated product, 1,2,3-benzenetriol, also known as pyrogallol (Fig. 6A). 1,2,3-Benzenetriol is known to undergo spontaneous oxidation in air (35, 36), and our cultures are vigorously shaken to provide a continuous supply of oxygen for the dioxygenase reaction. These oxidation products absorb at varying wavelengths, which leads to dark-colored microbiological medium (37, 38).

To follow pyrogallol formation and decomposition, we used UV-visible (UV-vis) spectroscopy of biological material in comparison to standard pyrogallol and purpurogallin (Fig. 6B and C; see also Fig. S9 and S10). Pyrogallol, prior to oxidation, absorbs

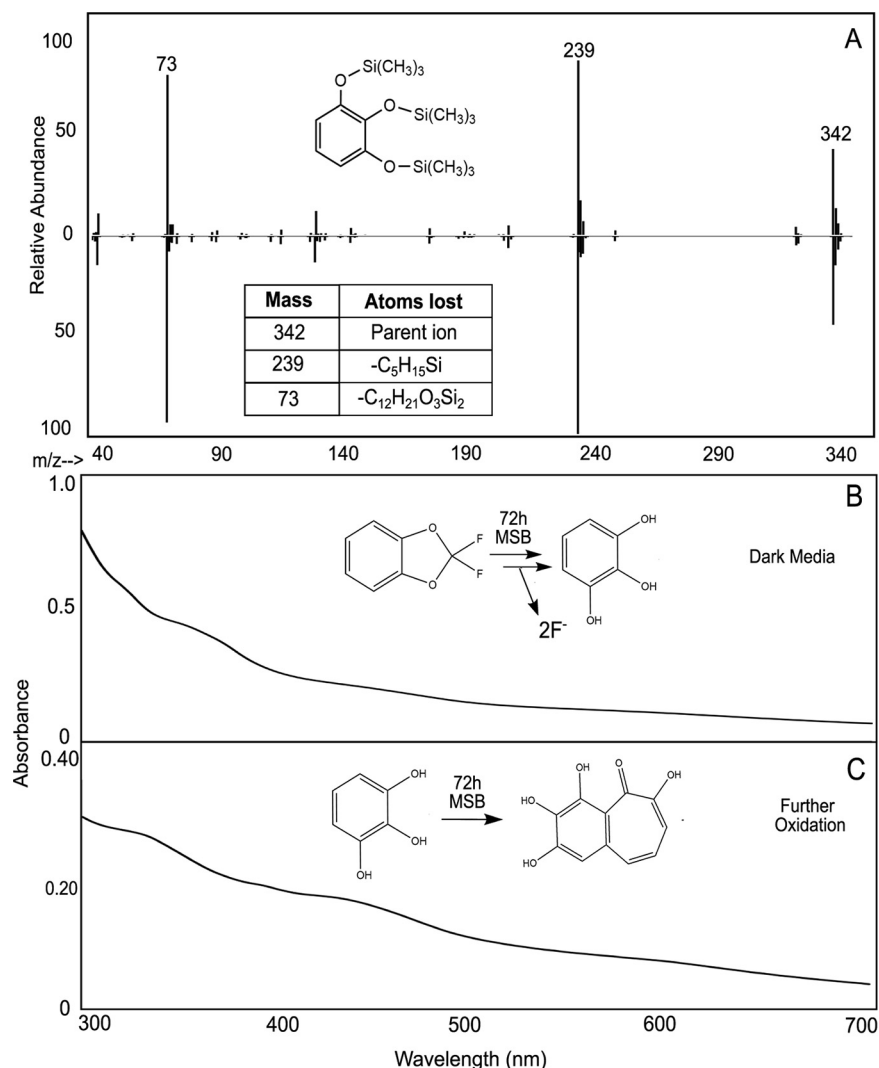


FIG 6 Evidence for the defluorinated aromatic product, pyrogallol, or 1,2,3-benzenetriol. (A) Mass spectrometry fragmentation pattern of derivatized 1,2,3-benzenetriol found in cell cultures from *E. coli* pDTG601a (top) compared to standard derivatized 1,2,3-benzenetriol (bottom). (B) UV-vis spectrum of *E. coli* pDTG601a cell culture supernatant after incubation with DFBD for 72 h. (C) UV-vis spectrum of standard 1,2,3-benzenetriol in MSB medium after 72 h. Time course data are shown in Fig. S10.

only below 300 nm, which is difficult to analyze because DFBD absorbs in the 250- to 300-nm region. So, we analyzed at wavelengths above 300 nm. When added to sterile growth medium, pyrogallol quickly oxidized to a species that absorbs at 320 nm, purportedly purpurogallin (Fig. S10). Over time, this decayed with the appearance of absorbance at 420 to 440 nm, indicating the formation of purpurogallin-quinone (35). Over time, other absorbing species led to the previously described brown to black coloration of pyrogallol medium that was observed here with DFBD in medium in the presence of toluene dioxygenase (Fig. 6B) and standard pyrogallol in medium (Fig. 6C).

Mechanism of defluorination. A satisfactory explanation for DFBD defluorination had to align several key data. First, fluoride release was immediate and rapid and required toluene-grown cells, and medium darkening lagged temporally. All bacterial strains expressing toluene dioxygenase, even singly, released fluoride and darkened medium. However, known further transformation products of the toluene dioxygenase, which are 4,5-DD-DFBD and the phenols and catechols characterized here, did not undergo defluorination. Indeed, the presence of the enzyme dihydrodiol dehydrogenase, which

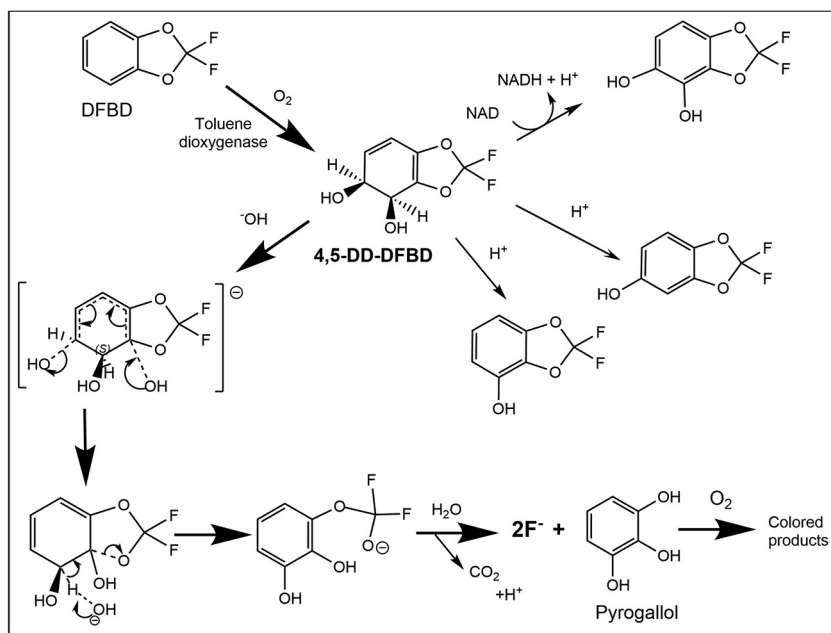


FIG 7 Scheme showing 2,2-difluoro-1,3-benzodioxole (DFBD) oxidation by toluene dioxygenase to 4,5-dihydroxy-DFBD (4,5-DD-DFBD) and subsequent reactions producing fluoride ion and dark medium. The major path is highlighted by darker arrows. The three intermediates between 4,5-DD-DFBD and fluoride plus pyrogallol are expected to have a very short lifetime, cannot be demonstrated directly, and represent a proposed mechanism for fluoride and medium darkening. The minor products on the upper right are stable and were demonstrated in this work, as was pyrogallol and the pathway for color formation.

transformed at least some 4,5-DD-DFBD to the corresponding catechol, diminished fluoride release and color formation. Those observations, together with the immediate fluoride release, indicated that 4,5-DD-DFBD was undergoing another reaction, and that reaction was fast enough to compete with the dehydrogenase kinetically. This previously undescribed reaction pathway had to explain rapid fluoride release, pyrogallol appearance in the medium, and a lag in darkening of the medium.

It was not possible to isolate and store 4,5-DD-DFBD due to its extreme instability compared to other bicyclic dihydrodiols (34). Its instability was presumably linked to the highly electron-withdrawing $-\text{OCF}_2-$ moiety adjacent to the dihydrodiol group, precisely the atoms that are lost (Fig. 7). The carbon atom linking the two groups referred to above is a bridgehead carbon. This bridgehead carbon would be highly susceptible to nucleophilic attack by a hydroxide anion in solution. The resultant trihydroxy compound (middle left, Fig. 7) is expected to decompose with C-O breakage, rearomatization, and opening of the five-membered 1,3-dioxole ring. We propose here that these are spontaneous reactions, driven by the electrophilicity of the bridgehead carbon atom and the stabilization energy inherent in rearomatization that occurs with C-O bond cleavage. However, we cannot rule out the possibility of a cell component assisting in hydroxide attack on the bridgehead carbon. Once the C-O bond cleaves, the resultant $-\text{OCF}_2\text{O}-$ moiety is highly unstable, to undergo very rapid hydrolysis to produce carbon dioxide and the two fluorine atoms as fluoride. Pyrogallol, the other product, is not colored but over time will oxidize to a range of colored products that darken the medium (Fig. 7).

Potential for DFBD defluorination by other aromatic oxygenase-containing bacteria. A question naturally arises as to whether DFBD defluorination by this mechanism is common, since genes encoding the oxygenation of toluene and other aromatic hydrocarbons are widespread in bacterial genomes (39–41). In addition to dioxygenation, many bacteria oxidize toluene via monooxygenases (39). Given the stability of monohydroxy and catecholic DFBD metabolites, we did not expect strains with monooxygenases to defluorinate DFBD. To test this hypothesis, *Burkholderia cepacia* G4,

TABLE 1 Homologs of the toluene dioxygenase alpha-subunit ([WP_012052601.1](#)) with high sequence identity over the majority of the sequence length^a

Percent identity	No. of sequences	Query sequence coverage
100%	6	100%
>90%	9	100%
>80%	19	>97%
>70%	51	>96%
>60%	177	>96%
>50%	293	>95%

^aThe sequences searched were compiled from three sources: *Pseudomonas* genome database, RHObase database, and NCBI nonredundant protein database. Percent identity was determined by pairwise BLAST (49), and the query sequence coverage refers to the extent over which the two sequences aligned.

containing toluene-2-monoxygenase, was grown on glucose and induced with toluene. After 24 h of incubation with DFBD, this strain did not release fluoride or create a dark color in the medium.

Dioxygenases that oxidize multiring substrates were considered to be better candidates to test for DFBD defluorination. Defluorination and darkening of the medium were not observed with *Pseudomonas* sp. strain NCIB 9816 or *Pseudomonas* sp. strain 9816-11, each of which expresses a naphthalene dioxygenase. Biphenyl dioxygenases that have different amino acid sequences were also tested with two bacteria, *Burkholderia xenovorans* LB400 and *Sphingobium yanoikuyae* B1. After induction with biphenyl and incubation with DFBD for 24 h, no fluoride release or color change was observed with either strain.

Identifying enzymes with greater similarity to the toluene dioxygenase from *P. putida* F1. Toluene dioxygenase is known to be a Rieske oxygenase, a very common class of proteins in aerobic bacteria (39–41). The Rieske oxygenases are composed of two protein subunits. The cofactors and the active site are within the larger, or alpha-, subunit. The alpha-subunit contains a Rieske iron sulfur cluster and a mononuclear iron center. Since the alpha-subunit of Rieske dioxygenases determines substrate specificity (42, 43), sequence comparisons with this subunit are most germane to the question as to which enzymes and organisms will defluorinate DFBD.

The amino acid sequence of the *P. putida* F1 toluene dioxygenase alpha-subunit ([WP_012052601.1](#)) was used to search the *Pseudomonas* genome database (22, 23) for homologs to the alpha-subunit of toluene dioxygenase on 6 August 2021 using DIAMOND-BLAST. The closer the sequence to the toluene dioxygenase studied here, the more likelihood that the active site would bind and oxygenate DFBD in a manner leading to defluorination (Table 1). This search identified proteins with amino acid sequences that were 100% identical in the following *Pseudomonas* strains with the locus tags given in the parentheses: *Pseudomonas monteilii* SB3101 (X970_10585), *P. monteilii* SB3078 (X969_10930), *P. putida* YKD221 (TR32_RS03575), *Pseudomonas* sp. strain NBRC 111125 (APH29_RS14695), and *P. putida* UV4/95 (CBP06_RS10555). Published substrate specificity studies with *P. putida* UV4/95 have shown the same substrate spectrum as *P. putida* F1 (44), consistent with the 100% sequence identity of the dioxygenase alpha-subunits.

Next, we queried the RHObase, or [Ring-Hydroxylating Oxygenase database](#), which focuses specifically on characterized Rieske oxygenases using the term “toluene dioxygenase” on 7 August 2021. This identified several enzymes denoted as toluene dioxygenase or nitrotoluene dioxygenases. One of these, from *Pseudomonas putida* DOT-T1E ([ADI95397](#)), was 100% identical to the alpha-subunit of toluene dioxygenase from *P. putida* F1.

The large GenBank nonredundant database, with 419,490,021 sequences as of 6 August 2021, was searched to determine the approximate number of homologs and particularly close sequence matches. A BLAST search yielded over 1,200 homologous sequences with an E value lower than e^{-50} , indicating they matched extremely well. Of those, 293 showed sequence identity of >50% and 9 showed sequence identity of

TABLE 2 Bacterial strains used, growth conditions selected, and known enzymes expressed under the conditions specified

Bacterial strain	Growth substrate/ inducer	Relevant enzyme(s) expressed ^a	Reference(s)
<i>Pseudomonas putida</i> F1	L-Arginine	Toluene metabolism enzymes at very low levels	52
<i>Pseudomonas putida</i> F1	Toluene	Toluene pathway and regulatory proteins	52
<i>Pseudomonas putida</i> F39/D	Toluene	All toluene pathway enzymes with mutation in the diol dehydrogenase (TodD)	48
<i>Escherichia coli</i> K-12 ^b	D-Glucose	NA ^d	
<i>Escherichia coli</i> JM109 (pDTG601a)	IPTG ^c	Toluene dioxygenase	29
<i>Escherichia coli</i> JM109 (pDTG602)	IPTG ^c	Toluene dioxygenase and diol dehydrogenase	29
<i>Pseudomonas</i> sp. NCIB 9816	Naphthalene	Naphthalene dioxygenase pathway	53, 54
<i>Pseudomonas</i> sp. NCIB 9816-11	Naphthalene	Naphthalene enzymes with diol dehydrogenase mutation	53, 54
<i>Burkholderia cepacia</i> G4	Toluene	Toluene-2-monoxygenase pathway	55
<i>Sphingobium yanoikuyae</i> B1	Biphenyl	Biphenyl dioxygenase pathway	56
<i>Paraburkholderia xenovorans</i> LB400	Biphenyl	Biphenyl dioxygenase pathway	57

^aBased on peer-reviewed references.

^bNo aromatic ring oxygenases known to us induced with *E. coli* grown on glucose.

^cIPTG, isopropyl- β -D-1-thiogalactopyranoside; added to induce expression of the specified enzyme(s) indicated.

^dNA, not applicable.

>90% (Table 1). Closely related sequences are found in *Pseudomonas*, *Comamonas*, *Sphingomonas*, *Paraburkholderia*, *Nocardioideis*, and *Rhodococcus*.

Next, the Rieske dioxygenases in the bacteria that were tested here and found not to release fluoride were analyzed for amino acid sequence relatedness to the *P. putida* F1 toluene dioxygenase. The biphenyl dioxygenase from *Sphingobium yanoikuyae* B1 is 37% identical in amino acid sequence to toluene dioxygenase via pairwise BLAST alignment. The *Pseudomonas* sp. strain NCIB 9816 naphthalene dioxygenase is 32% identical to the toluene dioxygenase alpha-subunit. The *Paraburkholderia xenovorans* LB400 biphenyl dioxygenase is 65% identical.

It is not currently known how much a sequence might deviate from 100% identity, and if slightly different, what specific requirements would ensure reactivity with DFBD at the 4,5-position leading to defluorination. Further experimental work is warranted to test other bacteria with closely related Rieske dioxygenases. It is possible that docking and molecular dynamics simulations could also be done to predict enzyme reactivity and regioselectivity with DFBD (45, 46), but those detailed computational experiments are beyond the scope of the present study. A search of the Protein Data Bank for homologs of toluene dioxygenase yielded four distinct Rieske dioxygenases with X-ray structures and >64% sequence identity. Based on the bioinformatic data presented here and the wide diversity of bacteria known to express Rieske dioxygenases, we suggest that the DFBD moiety in natural environments might be subject to the type of metabolism revealed here with *P. putida* F1.

Conclusions. *Pseudomonas* strains and oxygenases have the potential to catalyze defluorination reactions in unexpected ways as demonstrated here. Previously, *Pseudomonas* sp. strain T-12 expressing toluene dioxygenase was shown to hydroxylate a carbon bearing a fluorine substituent, leading to defluorination by *gem* elimination (17). In this study, a difluorinated ether was shown to be defluorinated by *P. putida* F1 via a different mechanism but also demonstrated to be dependent upon toluene dioxygenase. Bioinformatic analyses strongly suggest that DFBD and its derivatives will undergo defluorination by dioxygenases found in other known *Pseudomonas* strains and in natural environments.

MATERIALS AND METHODS

Bacterial strains, growth, and manipulations. Bacteria, growth substrates, enzymes expressed, and references are compiled in Table 2. Further specific details on growth and manipulations are provided below. *Pseudomonas putida* F1 was grown on Luria-Bertani (LB) plates and then grown overnight on minimal salts basal medium (MSB) (47) with carbon supplied via a vapor bulb containing toluene, as previously described (48). This 10-ml culture was then added to an additional 25 ml of MSB, and the toluene bulb was replaced with a 2,2-difluoro-1,3-benzodioxole bulb. This flask was incubated at 30°C with shaking at 200 rpm. Aliquots of the culture were taken out at various time points. Samples intended for measuring fluoride release were centrifuged to remove cells, and the supernatant was removed and

placed into a clean tube. For photographs of color change, the medium aliquots were taken directly and then stored at -20°C to be photographed simultaneously. *Pseudomonas putida* F39/D was originally streaked onto an LB plate and grown at 28°C . For liquid cultures, this strain was grown on MSB and 0.2% (wt/vol) L-arginine. A saturated 10-ml culture of *P. putida* F39/D, grown overnight, was added to 200 ml of MSB and 0.2% (wt/vol) arginine and allowed to grow to log phase at 30°C . Once log phase was attained, the culture was induced with toluene for 1 h. After induction, the toluene bulb was replaced with a DFBD bulb. After 2 h of incubation with DFBD, the cells were pelleted, and the supernatant was removed.

E. coli pDTG601a was maintained on LB plates with $100\ \mu\text{g/ml}$ ampicillin at 37°C . For experimental use, it was grown overnight on LB with ampicillin liquid, cells were pelleted, and then the cells were resuspended in MSB, 0.2% (wt/vol) glucose, and $100\ \mu\text{g/ml}$ ampicillin. After growing at 37°C for 2 h, this strain was induced with 1 mM IPTG for 1 h. After induction, a DFBD vapor bulb was added to the flask and the culture was left to incubate for a further 2 h. *E. coli* pDTG602 cells were maintained on LB-ampicillin plates at 37°C . For experimental use, this strain was grown overnight on MSB medium with glucose and $100\ \mu\text{g/ml}$ ampicillin. This overnight culture was used to inoculate a culture of 50 ml of MSB, glucose, and ampicillin and induced with IPTG for 1 h. After induction, DFBD was added in vapor form. Aliquots were taken at various time points and left to incubate overnight. *Pseudomonas* sp. NCIB 9816 and 9816-11 were maintained on LB plates at 28°C . NCIB 9816 was grown to log phase on 100 ml of MSB and naphthalene for induction of naphthalene dioxygenase. Subsequently, the culture was filtered through glass wool to remove naphthalene crystals and a vapor bulb of DFBD was added to the culture. NCIB 9816-11 was grown on MSB medium and 15 mM pyruvate. This culture was added to 25 ml of MSB and induced with 0.2% naphthalene. This culture was also filtered through glass wool before adding the DFBD vapor bulb, and then the culture was left to incubate for 24 h. *Burkholderia cepacia* G4 was maintained on LB plates at 28°C . It was grown in MSB and 0.2% glucose overnight. This culture was added to 25 ml of MSB and induced with toluene for 1 h. *Sphingobium yanoikuyae* B1 was maintained on LB plates at 28°C . Overnight, this strain was grown on MSB and biphenyl, which induces the biphenyl dioxygenase. *Paraburkholderia xenovorans* LB400 was maintained on nutrient agar plates at 28°C . Overnight, this strain was grown on MSB and biphenyl, which induces the biphenyl dioxygenase enzyme.

Chemicals. 2,2-Difluoro-1,3-benzodioxole (DFBD) was purchased from Matrix Scientific and $^1\text{H-NMR}$ indicated 97% purity. 2,2-Difluoro-1,3-benzodioxole-4-ol and 2,2-difluoro-1,3-benzodioxole-5-ol were from AstaTech with 95% purity. 1,2,3-Benzenetriol was purchased from Mallinckrodt with a purity of $\sim 95\%$. Purpurogallin was from Cayman Chemical and had a purity of 95%, as determined by $^1\text{H-NMR}$. *N, O*-Bis(trimethylsilyl)trifluoroacetamide was purchased from Fluka Analytical and had a purity of 99%. CDCl_3 and CD_3CN were obtained from Cambridge Isotope Laboratories, Inc., and had $>99\%$ purity. Methyl-*tert*-butyl ether (MTBE) and ethyl acetate (EtOH), solvents used for GC-MS, were from Sigma-Aldrich, both high-performance liquid chromatography (HPLC) grade, $>99\%$ pure. Toluene used for specified cell growth and induction was from Fisher Chemical and is 99% pure. Sodium fluoride (NaF) used for fluoride standards was obtained from Aldrich Chemical company, 99% pure. D-Glucose, used for growth of *E. coli* recombinant strains, was purchased from Sigma-Aldrich and was 99.5% pure. IPTG was obtained from Gold Bio. L-Arginine, used for growth of *Pseudomonas* strains, is from Calbiochem. Sodium pyruvate is from Alfa-Aesar with a purity of 99%. Biphenyl was from Spectrum Chemical and had a purity of 99%. Naphthalene was from Alfa-Aesar with a purity of 99%.

Nuclear magnetic resonance (NMR) experiments. Cell culture supernatants from both *E. coli* pDTG601a and *P. putida* F39/D after incubation with DFBD were extracted with an equal volume of ethyl acetate (EtOAc). In each case, the aqueous layer was drawn off and the organic layer was dried (MgSO_4), transferred to a round-bottom flask, and rotary evaporated. The residue was taken into CD_3CN for initial $^1\text{H-}$ and $^{19}\text{F-NMR}$ acquisitions on a Varian INOVA 500-MHz NMR spectrometer. The initial $^1\text{H-NMR}$ spectra were too complex to identify signals due to 4,5-dihydro-DFBD-4,5-diol, but $^{19}\text{F-NMR}$ (376 MHz, Fig. 3C; see also Fig. S6 in the supplemental material for CD_3CN) shows a clean AB pattern: 46.65 ppm (d, $J = 110.8$ Hz) and -49.05 ppm (d, $J = 110.8$ Hz) for the CF_2 fluorine atoms.

Cell culture supernatants from *E. coli* pDTG602 were extracted with MTBE, dried with anhydrous MgSO_4 , and then rotary evaporated. Subsequently, the CD_3CN solutions were concentrated and then directly dissolved in CDCl_3 . The products were as follows: $^1\text{H-NMR}$ (400 MHz, CDCl_3), 1,2,3-benzenetriol; 6.68 ppm (t, $J = 8.0$ Hz), 6.48 ppm (d, $J = 8.2$ Hz), 5.24 ppm (bs), 5.17 ppm (bs), and DFBD-ols, 6.57 ppm (d, $J = 8.4$ Hz), 6.51 ppm (d, $J = 8.4$ Hz), and buried OH broad singlets, $^{19}\text{F-NMR}$ (400 MHz, CDCl_3), -50.31 ppm (s), CF_2 . In the proton NMR, the high field doublet at 6.51 ppm is partly buried in a neighboring peak. Additional significant peaks that do not describe the 4,5-DD-DFBD are shown to be 1,2,3-benzenetriol (Fig. S7 and S9).

GC-MS experiments. For gas chromatography and mass spectrometry (GC-MS), cell culture supernatants were extracted with methyl-*tert*-butyl ether (MTBE). Equal volumes of organic and aqueous phases were used. Extraction was done directly in glass GC vials, which were shaken vigorously, and then the organic layer was drawn off and placed in a clean vial. One microliter of derivatizing agent, *N, O*-bis(trimethylsilyl)trifluoroacetamide, was added to each extracted sample. Product ion spectra were identified in positive ion mode on an HP6890 gas chromatograph with an HP5973 MS detector. GC conditions were as follows: helium gas, 1 ml/min; HP-1ms column (100% dimethylpolysiloxane capillary; 30 m by $250\ \mu\text{m}$ by $0.25\ \mu\text{m}$); starting temperature 50°C with a ramp of $10^{\circ}\text{C}/\text{min}$ to 320°C . Standards run on the GC-MS used the same program specified above. 2,2-Difluoro-1,3-benzodioxole-5-ol and 2,2-difluoro-1,3-benzodioxole-4-ol were prepared by placing a small volume of each into separate GC vials with $500\ \mu\text{l}$ of MTBE. One microliter of the derivatizing agent was added to each vial. Pyrogallol (1,2,3-benzenetriol)

was prepared similarly, by putting a small solid amount of the compound into 500 μ l of MTBE and adding 1 μ l of derivatizing agent.

Fluoride measurements. Fluoride ion measurements were determined using an ISE Ionplus Sure-Flow Orion fluoride probe from Thermo Fisher and the Orion Star A214 meter. To perform fluoride measurements, 1 ml of cell culture was pelleted. The supernatant was removed and placed into a 5-ml tube with 1 ml of TISAB (58.5 g/liter NaCl, 15 g/liter CH₃COOH, 66 g/liter CH₃COONa, and 1 g/liter 1,2-cyclohexane diaminetetraacetic acid). Calibrations of the probe were made with standard concentrations ranging from 10⁻⁵ M to 10⁻² M. Two standards were required for calibration. Standards were made with sodium fluoride in MSB medium.

UV-vis spectroscopy. UV-vis absorption scans were performed on a Cary 3500 double-beam UV-vis spectrophotometer containing a Xenon flash lamp from Agilent. Measurements of supernatant from an *E. coli* pDTG601a culture were taken after 72 h of incubation with DFBD. An aliquot was taken from the cell culture and pelleted to remove cells. The supernatant was removed and placed in a 1.5-ml disposable cuvette. The sample was then measured (300 to 700 nm) in increments of 5 nm. Standard 1,2,3-benzenetriol was prepared to a concentration of 0.1 M in water. To scan this compound, 1 ml of MSB was placed in a 1.5-ml disposable cuvette and 1,2,3-benzenetriol stock solution was added to a final concentration of 0.1 mM. This cuvette of MSB and 0.1 mM pyrogallol was left to sit at room temperature for 72 h and measured after that.

Bioinformatic methods. BLAST was used to query the NCBI GenBank nonredundant database (49). DIAMOND-BLAST was used to query the *Pseudomonas* genome database (50). The RHObase, or Ring-Hydroxylating Oxygenase database, was queried with a word search (51). All hits obtained from the searches were compiled manually. Comparisons with toluene dioxygenase and other single enzymes were carried out using pairwise BLAST (49) on the National Center for Biotechnology Information server.

SUPPLEMENTAL MATERIAL

Supplemental material is available online only.

FIG S1, PDF file, 0.1 MB.

FIG S2, PDF file, 0.1 MB.

FIG S3, PDF file, 0.1 MB.

FIG S4, PDF file, 0.1 MB.

FIG S5, PDF file, 0.1 MB.

FIG S6, PDF file, 0.1 MB.

FIG S7, PDF file, 0.1 MB.

FIG S8, PDF file, 0.1 MB.

FIG S9, PDF file, 0.1 MB.

FIG S10, PDF file, 0.2 MB.

ACKNOWLEDGMENTS

We thank Becky Parales for providing the recombinant *E. coli* strains: *E. coli* pDTG601a and *E. coli* pDTG602. We acknowledge Thomas Niehaus for making available the Cary spectrophotometer. We acknowledge Mikael Elias and Amir Shimon for helpful discussion about this project.

This project was funded by MnDRIVE Environment.

L.P.W., K.G.A., and M.D.B. conceived and designed the experiments. M.D.B., K.G.A., and J.E.R. performed the experiments. M.D.B., K.G.A., J.E.R., and L.P.W. analyzed the data. B.P. and T.N. contributed reagents/materials/analysis tools. M.D.B., K.G.A., and L.P.W. wrote the paper. All authors edited and approved the manuscript.

REFERENCES

- Sunderland EM, Hu XC, Dassuncao C, Tokranov AK, Wagner CC, Allen JG. 2019. A review of the pathways of human exposure to poly- and perfluoroalkyl substances (PFASs) and present understanding of health effects. *J Expo Sci Environ Epidemiol* 29:131–147. <https://doi.org/10.1038/s41370-018-0094-1>.
- Key BD, Howell RD, Criddle CS. 1997. Fluorinated organics in the biosphere. *Environ Sci Technol* 31:2445–2454. <https://doi.org/10.1021/es961007c>.
- Harper DB, O'Hagan D. 1994. The fluorinated natural products. *Nat Prod Rep* 11:123–133. <https://doi.org/10.1039/np9941100123>.
- Murphy CD, Schaffrath C, O'Hagan D. 2003. Fluorinated natural products: the biosynthesis of fluoroacetate and 4-fluorothreonine in *Streptomyces cattleya*. *Chemosphere* 52:455–461. [https://doi.org/10.1016/S0045-6535\(03\)00191-7](https://doi.org/10.1016/S0045-6535(03)00191-7).
- Smart B. 2001. Fluorine substituent effects (on bioactivity). *J Fluor Chem* 109:3–11. [https://doi.org/10.1016/S0022-1139\(01\)00375-X](https://doi.org/10.1016/S0022-1139(01)00375-X).
- O'Hagan D. 2008. Understanding organofluorine chemistry. An introduction to the C-F bond. *Chem Soc Rev* 37:308–319. <https://doi.org/10.1039/b711844a>.
- Liu Z, Bentel MJ, Yu Y, Ren C, Gao J, Pulikkal VF, Sun M, Men Y, Liu J. 2021. Near-quantitative defluorination of perfluorinated and fluorotelomer carboxylates and sulfonates with integrated oxidation and reduction. *Environ Sci Technol* 55:7052–7062. <https://doi.org/10.1021/acs.est.1c00353>.
- Huang S, Jaffé PR. 2019. Defluorination of perfluorooctanoic acid (PFOA) and perfluorooctane sulfonate (PFOS) by *Acidimicrobium sp.* strain A6. *Environ Sci Technol* 53:11410–11419. <https://doi.org/10.1021/acs.est.9b04047>.
- Murphy CD. 2016. Microbial degradation of fluorinated drugs: biochemical pathways, impacts on the environment and potential applications. *Appl Microbiol Biotechnol* 100:2617–2627. <https://doi.org/10.1007/s00253-016-7304-3>.

10. Müller K, Faeh C, Diederich F. 2007. Fluorine in pharmaceuticals: looking beyond intuition. *Science* 317:1881–1886. <https://doi.org/10.1126/science.1131943>.
11. Newton JJ, Brooke AJ, Duhamel B, Pulfer JM, Britton R, Friesen CM. 2020. Fluorodesulfurization of thionobenzodioxoles with silver(I) fluoride. *J Org Chem* 85:13298–13305. <https://doi.org/10.1021/acs.joc.0c01729>.
12. Thomas KA, Hand LH. 2012. Assessing the metabolic potential of phototrophic communities in surface water environments: fludioxonil as a model compound. *Environ Toxicol Chem* 31:2138–2146. <https://doi.org/10.1002/etc.1928>.
13. Alexandrino DAM, Mucha AP, Almeida CMR, Carvalho MF. 2020. Microbial degradation of two highly persistent fluorinated fungicides - epoxiconazole and fludioxonil. *J Hazard Mater* 394:122545. <https://doi.org/10.1016/j.jhazmat.2020.122545>.
14. Yu Y, Zhang K, Li Z, Ren C, Chen J, Lin YH, Liu J, Men Y. 2020. Microbial cleavage of C-F bonds in two C6 per- and polyfluorinated compounds via reductive defluorination. *Environ Sci Technol* 54:14393–14402. <https://doi.org/10.1021/acs.est.0c04483>.
15. Wang Y, Liu A. 2020. Carbon-fluorine bond cleavage mediated by metalloenzymes. *Chem Soc Rev* 49:4906–4925. <https://doi.org/10.1039/c9cs00740g>.
16. Xie Y, Chen G, May AL, Yan J, Brown LP, Powers JB, Campagna SR, Löffler FE. 2020. *Pseudomonas* sp. strain 273 degrades fluorinated alkanes. *Environ Sci Technol* 54:14994–15003. <https://doi.org/10.1021/acs.est.0c04029>.
17. Renganathan V. 1989. Possible involvement of toluene-2,3-dioxygenase in defluorination of 3-fluoro-substituted benzenes by toluene-degrading *Pseudomonas* sp. strain T-12. *Appl Environ Microbiol* 55:330–334. <https://doi.org/10.1128/aem.55.2.330-334.1989>.
18. Bondar VS, Boersma MG, Golovlev EL, Vervoort J, Van Berkel WJH, Finkelstein ZI, Solyanikova IP, Golovleva LA, Rietjens IMCM. 1998. ¹⁹F NMR study on the biodegradation of fluorophenols by various *Rhodococcus* species. *Biodegradation* 9:475–486. <https://doi.org/10.1023/A:1008391906885>.
19. Ferreira MI, Iida T, Hasan SA, Nakamura K, Fraaije MW, Janssen DB, Kudo T. 2009. Analysis of two gene clusters involved in the degradation of 4-fluorophenol by *Arthrobacter* sp. strain IF1. *Appl Environ Microbiol* 75:7767–7773. <https://doi.org/10.1128/AEM.00171-09>.
20. Fox BG, Borneman JG, Wackett LP, Lipscomb JD. 1990. Haloalkene oxidation by the soluble methane monooxygenase from *Methylosinus trichosporium* OB3b: mechanistic and environmental implications. *Biochemistry* 29:6419–6427. <https://doi.org/10.1021/bi00479a013>.
21. Che S, Jin B, Liu Z, Yu Y, Liu J, Men Y. 2021. Structure-specific aerobic defluorination of short-chain fluorinated carboxylic acids by activated sludge communities. *Environ Sci Technol Lett* 8:668–674. <https://doi.org/10.1021/acs.estlett.1c00511>.
22. Goldman P. 1965. The enzymatic cleavage of the carbon-fluorine bond in fluoroacetate. *J Biol Chem* 240:3434–3438. [https://doi.org/10.1016/S0021-9258\(18\)97236-4](https://doi.org/10.1016/S0021-9258(18)97236-4).
23. Alexandrino DAM, Ribeiro I, Pinto LM, Cambra R, Oliveira RS, Pereira F, Carvalho MF. 2018. Biodegradation of mono-, di- and trifluoroacetate by microbial cultures with different origins. *N Biotechnol* 43:23–29. <https://doi.org/10.1016/j.nbt.2017.08.005>.
24. Nagata Y, Nariya T, Ohtomo R, Fukuda M, Yano K, Takagi M. 1993. Cloning and sequencing of a dehalogenase gene encoding an enzyme with hydrolyase activity involved in the degradation of gamma-hexachlorocyclohexane in *Pseudomonas paucimobilis*. *J Bacteriol* 175:6403–6410. <https://doi.org/10.1128/jb.175.20.6403-6410.1993>.
25. Strotmann UJ, Pentenga M, Janssen DB. 1990. Degradation of 2-chloroethanol by wild type and mutants of *Pseudomonas putida* US2. *Arch Microbiol* 154:294–300. <https://doi.org/10.1007/BF00248970>.
26. Winsor GL, Van Rossum T, Lo R, Khaira B, Whiteside MD, Hancock RE, Brinkman FS. 2009. *Pseudomonas* Genome Database: facilitating user-friendly, comprehensive comparisons of microbial genomes. *Nucleic Acids Res* 37:D483–D488. <https://doi.org/10.1093/nar/gkn861>.
27. Winsor GL, Griffiths EJ, Lo R, Dhillon BK, Shay JA, Brinkman FS. 2016. Enhanced annotations and features for comparing thousands of *Pseudomonas* genomes in the *Pseudomonas* genome database. *Nucleic Acids Res* 44:D646–D653. <https://doi.org/10.1093/nar/gkv1227>.
28. Reardon KF, Mosteller DC, Bull Rogers JD. 2000. Biodegradation kinetics of benzene, toluene, and phenol as single and mixed substrates for *Pseudomonas putida* F1. *Biotechnol Bioeng* 69:385–400. [https://doi.org/10.1002/1097-0290\(20000820\)69:4<385::AID-BIT5>3.0.CO;2-Q](https://doi.org/10.1002/1097-0290(20000820)69:4<385::AID-BIT5>3.0.CO;2-Q).
29. Zylstra GJ, McCombie WR, Gibson DT, Finette BA. 1988. Toluene degradation by *Pseudomonas putida* F1: genetic organization of the tod operon. *Appl Environ Microbiol* 54:1498–1503. <https://doi.org/10.1128/aem.54.6.1498-1503.1988>.
30. Kasahara Y, Morimoto H, Kuwano M, Kadoya R. 2012. Genome-wide analytical approaches using semi-quantitative expression proteomics for aromatic hydrocarbon metabolism in *Pseudomonas putida* F1. *J Microbiol Methods* 91:434–442. <https://doi.org/10.1016/j.mimet.2012.09.017>.
31. Leahy JG, Olsen RH. 2006. Kinetics of toluene degradation by toluene-oxidizing bacteria as a function of oxygen concentration, and the effect of nitrate. *FEMS Microbiol Ecol* 23:23–30. <https://doi.org/10.1111/j.1574-6941.1997.tb00387.x>.
32. Finette BA, Gibson DT. 1988. Initial studies on the regulation of toluene degradation by *Pseudomonas putida* F1. *Biocatal Biotransformation* 2:29–37. <https://doi.org/10.3109/10242428808998177>.
33. Williams MG, Olson PE, Tautvydas KJ, Bitner RM, Mader RA, Wackett LP. 1990. The application of toluene dioxygenase in the synthesis of acetylene-terminated resins. *Appl Microbiol Biotechnol* 34:316–321. <https://doi.org/10.1007/BF00170050>.
34. Wackett LP, Kwart LD, Gibson DT. 1988. Benzylic monooxygenation catalyzed by toluene dioxygenase from *Pseudomonas putida*. *Biochemistry* 27:1360–1367. <https://doi.org/10.1021/bi00404a041>.
35. Abrash HI, Shih D, Elias W, Malekmehr F. 1989. A kinetic study of the air oxidation of pyrogallol and purpurogallin. *Int J Chem Kinet* 21:465–476. <https://doi.org/10.1002/kin.550210609>.
36. Ramasarma T, Rao AVS, Devi MM, Omkumar RV, Bhagyashree KS, Bhat SV. 2015. New insights of superoxide dismutase inhibition of pyrogallol autoxidation. *Mol Cell Biochem* 400:277–285. <https://doi.org/10.1007/s11010-014-2284-z>.
37. Yoshida H, Yamada H. 1985. Microbial production of pyrogallol through decarboxylation of gallic acid. *Agric Biol Chem* 49:659–663. <https://doi.org/10.1271/bbb1961.49.659>.
38. Osawa R, Walsh T. 1995. Detection of bacterial gallate decarboxylation by visual color discrimination. *J Gen Appl Microbiol* 41:165–170. <https://doi.org/10.2323/jgam.41.165>.
39. Jabłońska J, Tawfik DS. 2019. The number and type of oxygen-utilizing enzymes indicates aerobic vs. anaerobic phenotype. *Free Radic Biol Med* 140:84–92. <https://doi.org/10.1016/j.freeradbiomed.2019.03.031>.
40. Ferraro DJ, Gakhar L, Ramaswamy S. 2005. Rieske business: structure-function of Rieske non-heme oxygenases. *Biochem Biophys Res Commun* 338:175–190. <https://doi.org/10.1016/j.bbrc.2005.08.222>.
41. Wackett LP. 2002. Mechanism and applications of Rieske non-heme iron dioxygenases. *Enzyme Microb Technol* 31:577–587. [https://doi.org/10.1016/S0141-0229\(02\)00129-1](https://doi.org/10.1016/S0141-0229(02)00129-1).
42. Parales JV, Parales RE, Resnick SM, Gibson DT. 1998. Enzyme specificity of 2-nitrotoluene 2,3-dioxygenase from *Pseudomonas* sp. strain J542 is determined by the C-terminal region of the alpha subunit of the oxygenase component. *J Bacteriol* 180:1194–1199. <https://doi.org/10.1128/JB.180.5.1194-1199.1998>.
43. Parales RE, Lee K, Resnick SM, Jiang H, Lessner DJ, Gibson DT. 2000. Substrate specificity of naphthalene dioxygenase: effect of specific amino acids at the active site of the enzyme. *J Bacteriol* 182:1641–1649. <https://doi.org/10.1128/JB.182.6.1641-1649.2000>.
44. Boyd DR, Sharma ND, Bowers NI, Dalton H, Garrett MD, Harrison JS, Sheldrake GN. 2006. Dioxygenase-catalysed oxidation of disubstituted benzene substrates: benzylic monohydroxylation versus aryl *cis*-dihydroxylation and the meta effect. *Org Biomol Chem* 4:3343–3349. <https://doi.org/10.1039/b608417f>.
45. Aukema KG, Escalante DE, Maltby MM, Bera AK, Aksan A, Wackett LP. 2017. *In silico* identification of bioremediation potential: carbamazepine and other recalcitrant personal care products. *Environ Sci Technol* 51:880–888. <https://doi.org/10.1021/acs.est.6b04345>.
46. Escalante DE, Aukema KG, Wackett LP, Aksan A. 2017. Simulation of the bottleneck controlling access into a Rieske active site: predicting substrates of naphthalene 1,2-dioxygenase. *J Chem Inf Model* 57:550–561. <https://doi.org/10.1021/acs.jcim.6b00469>.
47. Stanier RY, Palleroni NJ, Doudoroff M. 1966. The aerobic pseudomonads: a taxonomic study. *J Gen Microbiol* 43:159–271. <https://doi.org/10.1099/00221287-43-2-159>.
48. Gibson DT, Koch JR, Schulz CL, Kallio RE. 1968. Oxidative degradation of aromatic hydrocarbons by microorganisms. II. Metabolism of halogenated aromatic hydrocarbons. *Biochemistry* 7:3795–3802. <https://doi.org/10.1021/bi00851a003>.
49. Altschul S, Gish W, Miller W, Myers E, Lipman D. 1990. Basic local alignment search tool. *J Mol Biol* 215:403–410. [https://doi.org/10.1016/S0022-2836\(05\)80360-2](https://doi.org/10.1016/S0022-2836(05)80360-2).

50. Buchfink B, Xie C, Huson DH. 2015. Fast and sensitive protein alignment using DIAMOND. *Nat Methods* 12:59–60. <https://doi.org/10.1038/nmeth.3176>.
51. Chakraborty J, Jana T, Saha S, Dutta T. 2014. Ring-Hydroxylating Oxygenase database: a database of bacterial aromatic ring-hydroxylating oxygenases in the management of bioremediation and biocatalysis of aromatic compounds. *Environ Microbiol Rep* 6:519–523. <https://doi.org/10.1111/1758-2229.12182>.
52. Gibson D, Koch J, Kallio R. 1968. Oxidative degradation of aromatic hydrocarbons by microorganisms. I. Enzymic formation of catechol from benzene. *Biochemistry* 7:2653–2662. <https://doi.org/10.1021/bi00847a031>.
53. Davies JI, Evans WC. 1964. Oxidative metabolism of naphthalene by soil pseudomonads. The ring-fission mechanism. *Biochem J* 91:251–261. <https://doi.org/10.1042/bj0910251>.
54. Yang Y, Chen RF, Shiaris MP. 1994. Metabolism of naphthalene, fluorene, and phenanthrene: preliminary characterization of a cloned gene cluster from *Pseudomonas putida* NCIB 9816. *J Bacteriol* 176:2158–2164. <https://doi.org/10.1128/jb.176.8.2158-2164.1994>.
55. Folsom BR, Chapman PJ, Pritchard PH. 1990. Phenol and trichloroethylene degradation by *Pseudomonas cepacia* G4: kinetics and interactions between substrates. *Appl Environ Microbiol* 56:1279–1285. <https://doi.org/10.1128/aem.56.5.1279-1285.1990>.
56. Gibson DT. 1999. *Beijerinckia* sp strain B1: a strain by any other name. *J Ind Microbiol Biotechnol* 23:284–293. <https://doi.org/10.1038/sj.jim.2900715>.
57. Mondello FJ. 1989. Cloning and expression in *Escherichia coli* of *Pseudomonas* strain LB400 genes encoding polychlorinated biphenyl degradation. *J Bacteriol* 171:1725–1732. <https://doi.org/10.1128/jb.171.3.1725-1732.1989>.